

Correlation between Spin Polarization and Magnetic Moment in Ferromagnetic Alloys

Tat-Sang Choy, Jian Chen, and Selman Hershfield

*Department of Physics and National High Magnetic Field Laboratory,
University of Florida, Gainesville, FL 32611*

The correlation between the magnetic moment in ferromagnetic alloys and the tunneling spin polarization in ferromagnet-insulator-superconductor tunneling experiments has been a mystery. The measured spin polarization for Fe, Co, Ni, and various Ni alloys is positive and roughly proportional to their magnetic moments, which can not be explained by considering the net density of states. Using a tight-binding coherent potential approximation (CPA) model, we show that while the polarization of the net density of states is not correlated with the magnetic moment, the polarization of the density of states of s electrons is correlated with the magnetic moment in the same manner as observed by the tunneling experiments. We also discuss the spin polarization measurements by Andreev reflection experiments, some of which obtained different results from the tunneling experiments and our calculations.

PACS numbers: 75.70.-i, 75.10.Lp, 72.15.-v, 85.30.Mn

I. INTRODUCTION

There has been renewed interest in spin-polarized transport over the last decade. This interest comes in part because of a wide range of novel phenomena, e.g., the giant and colossal magnetoresistance,^{1,2} spin-injection experiments,³ and spin-polarized tunneling experiments.⁴⁻⁹ One of the most fundamental properties of spin polarized transport in a ferromagnet is the polarization in the density of states at the Fermi energy. This polarization enters either directly or indirectly into most transport calculations. In particular, since tunneling experiments measure the density of states, they should provide a direct measure of this polarization. In the case of ferromagnet-insulator-ferromagnet tunneling experiments one measures the product of the spin polarizations.⁵ However, in ferromagnet-insulator-superconductor tunneling experiments where the density of states in the superconductor is Zeeman split by a field in the plane of the film, one can in principle measure directly the spin polarization in the density of states.

Tedrow, Meservey, and collaborators carried out a series of ferromagnet-insulator-superconductor experiments on Fe, Co, Ni, and Ni alloys in the 1970's. They found two surprising results.¹⁰ First, the electron spin polarization for Fe, Co, and Ni is positive. Assuming the tunneling conductance to be proportional to the total density of states at the Fermi level, band structure calculations predict positive spin polarization for Fe and negative spin polarization for Co and Ni, even though these calculations have successfully explained the Slater-Pauling curve¹¹⁻¹⁴ for the magnetic moments. Second, the spin polarization for Fe, Co, Ni, and the Ni alloys is roughly proportional to the magnetic moments. On the other hand, it is expected that only electrons near the Fermi level participate in the tunneling process. Given the complicated band structure of the transition metals, it is not clear why the electron spin polarization measured by tunneling, a property of the Fermi surface, and

the magnetic moment, a property of the Fermi whole sea, are related in such a simple way.

Recently, Soulen *et al.*¹⁵ and Upadhyay *et al.*¹⁶ independently studied the spin polarization of ferromagnets with Andreev reflection point contact experiments. The values of the spin polarization measured in these experiments are different from those obtained in the tunneling experiments, although they are in the same range. For example, the spin polarization of Ni is 43-46.5% as measured by Soulen *et al.* and 32% as measured by Upadhyay *et al.*, while the tunneling spin polarization of Ni measured by Moodera *et al.* is 33%.⁸ The difference may be due to the experiments measuring related but different quantities. One may have to take into account the different dependencies on the density of states and the Fermi velocity for two sets of experiments.¹⁷ The discrepancies in the experiments indicates that it is important for a theory to compare the trend instead of particular values of the experiments. More recently, by using Andreev reflection techniques, Nadgorny *et al.*¹⁸ measured the spin polarization of $\text{Ni}_x\text{Fe}_{1-x}$ alloys to be about 45%, roughly independent of the magnetic moment. Their results are different from the tunneling measurements made by Tedrow and Meservey.

There have been a number of theoretical calculations to explain the results of Tedrow and Meservey's tunneling experiments. Many of these calculations concluded that the tunneling density of states is dominated by only a fraction of the electrons. In the work of Stearns¹⁹, the relevant electronic states are a t_{2g} -like band that is modeled by a parabolic dispersion near the Fermi surface. Hertz and Aoi²⁰ concluded that tunneling measures the s density of states as modified by many body effects due to the electron interaction with spin waves. Tsymbal and Pettifor²¹ studied the tunneling from Fe and Co by a tight-binding model which has only $ss\sigma$ bonds between the ferromagnet and the insulator. They concluded that only s electron tunneling was sufficient to explain the experiments. Recently, Nguyen-Manh *et al.*²² per-

formed a self-consistent band structure calculation of the Co/Al₂O₃ interface by a LMTO technique. Their calculation suggested that the interfacial cobalt *d* bands spin polarize *s-p* bands in the barrier, resulting in a positive tunneling spin polarization. On the other hand, Mazin¹⁷ and Nadgorny *et al.*¹⁸ suggested that spin polarization measured by both the tunneling and Andreev reflection experiments should be found from the polarization of the density of states times the Fermi velocity squared. The values of the polarization obtained from the all of the above models are in the same range of the experimental values; however, all these models are different and it is not clear which model is closer to reality.

To understand if there is indeed a subset of the electronic states which can account for the tunneling density of states, in this article we present a microscopic calculation for *both* the magnetic moment and the various density of states based on a self-consistent tight-binding coherent potential approximation (CPA)²³ model. In a range of alloys we find that the *s* density of states follows the same trend as the measured tunneling density of states. This is the first microscopic calculation to see this correlation. Furthermore, we are able to understand the correlation seen in our calculation and to show that it is not universal, i.e., the tunneling density of states is not simply proportional to the magnetic moment. There may even be some alloys where they are inversely correlated.

II. REVIEW OF EXPERIMENTS

In this section, we review the series of tunneling experiments by Tedrow and Meservey which show a correlation between the spin polarization and the magnetic moment. We also discuss the spin polarization measurements by Andreev reflection.

In the tunneling experiments of Tedrow and Meservey, spin polarized electrons tunnel from films made by alloying Ni and other 3*d* transition metals. In Fig. 1(a), the tunneling spin polarization for the Ni alloys is plotted against the average number of valence electrons per atom, which is changed by changing the composition of the alloys. Figure 1(a) looks very similar to the Slater-Pauling curve shown in Fig. 1(b), in which the bulk magnetic moment of alloys are plotted against the average number of valence electrons per atom. In NiFe and NiMn, the spin polarization peak is close to the magnetic moment peak. In NiCu, NiCr, and NiTi, both the spin polarization and the magnetic moment decrease monotonically as impurity concentrations increase. The thresholds at which the spin polarization and the magnetic moment drops to zero are close to each other. These similarities suggest that the spin polarization and the magnetic moment are correlated.

To see how the spin polarization relates to the magnetic moment, we follow Tedrow and Meservey¹⁰ and plot the spin polarization against the magnetic moment for

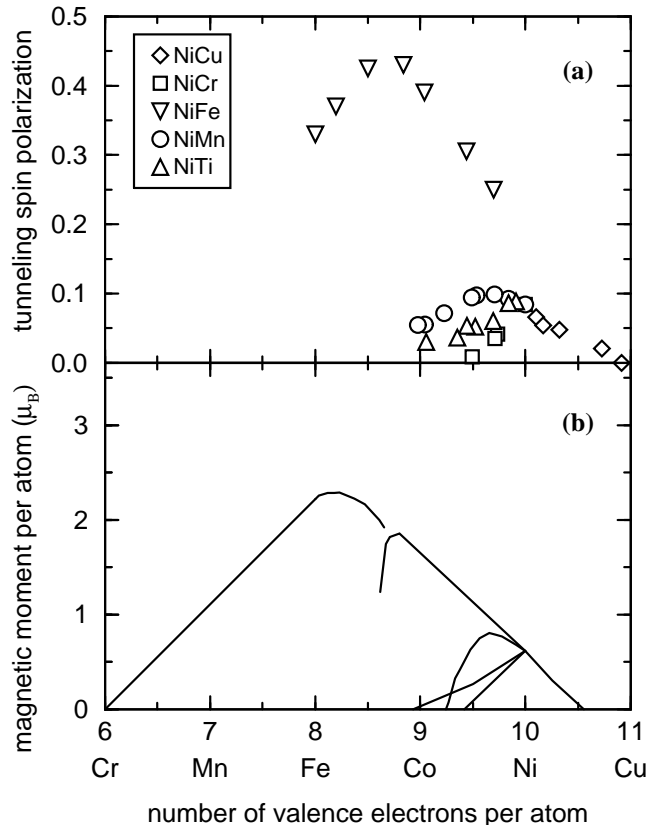


FIG. 1. Experimental data of (a) tunneling spin polarization and (b) bulk magnetic moment of 3*d* alloys versus the average number of valence electrons per atom. The similarities between (a) and (b) suggest the tunneling spin polarization and the magnetic moment are related.

NiCr, NiCu, NiMn, and NiTi in Fig. 2. The spin polarization data are taken from the experiment of Tedrow and Meservey, and the magnetic moment data are taken from the bulk measurements of alloys with the same compositions. Figure 2 shows a clear correlation between the spin polarization and the magnetic moment in these alloys. The data points for different alloys are roughly in a straight line passing through the origin.

Finite spin polarization is obtained for a few samples with zero bulk magnetic moments. This is probably due to the difference between the estimated bulk magnetic moments, which are taken from experiments on alloys with the same composition, and the surface magnetic moments of the actual sample, which are not measured in the tunneling experiments. When the magnetic moment is zero, there should be no difference between the majority and minority spins, the spin polarization is expected to be zero.

In Fig. 3, we plotted the tunneling data shown in Fig. 2 together with the tunneling measurements on other samples fabricated from different techniques by Tedrow and Meservey and by Moodera. Also included are the spin polarization measurements using Andreev reflection of Soulen *et al.*, Nadgorny *et al.*, and Upadhyay *et al.*

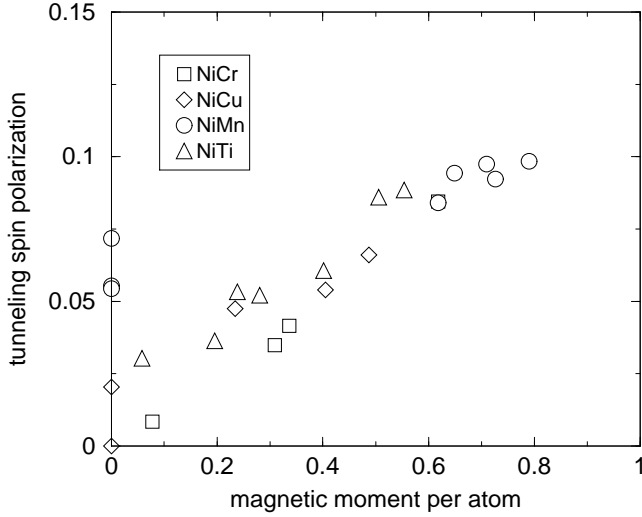


FIG. 2. Experimental tunneling spin polarization¹⁰ of NiCr, NiCu, NiMn, and NiTi versus the bulk magnetic moment of the corresponding alloy. The data points for different alloys roughly line in the same straight line. The commonly accepted experimental bulk magnetic moments of alloys are used as the x-coordinates. Finite spin polarization is obtained for zero magnetic moments in some samples. This is probably due to the difference between the bulk magnetic moments used on the graph and the surface magnetic moments of the actual samples, which are not measured. When the magnetic moment is zero, there should be no difference between the majority and minority spins, the spin polarization is expected to be zero.

The two dashed lines outline an area which roughly divides the graph into a fcc region (left) and a bcc region (right). When a data point is close to this area, the structure depends on the particular sample. One can visually identify three regimes in the figure: the lower left regime (fcc NiCr, NiCu, NiMn and NiTi), the middle regime (fcc NiFe with magnetic moment less than about $1.8 \mu_B$), and the right regime (bcc NiFe with magnetic moment greater than about $2 \mu_B$). There is a clear correlation between the spin polarization and the magnetic moment in the lower left regime, which is the same as Fig. 2. In the middle regime, the tunneling data and the Andreev reflection data by Upadhyay *et al.* only show a roughly increasing relation; on the other hand, the Andreev reflection data by Soulen *et al.* and Nadgorny *et al.* suggest that the spin polarization is independent of the magnetic moment. In right regime of Fig. 3, no clear correlation is seen between the spin polarization and the magnetic moment. However, this regime corresponds to the peak area near Fe in Fig. 1, which clearly indicates a correlation between the tunneling spin polarization and the magnetic moment.

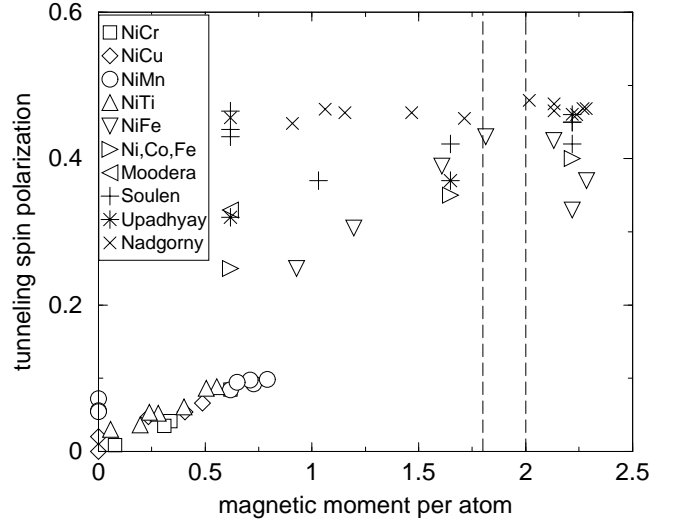


FIG. 3. Spin polarization obtained by different experiments versus the bulk magnetic moment of the corresponding alloy. The open symbols are tunneling data and the rest are obtained from Andreev reflection experiments. The two dashed lines outline an area which roughly divides the graph into a fcc region (left) and a bcc region (right).

III. MODEL

To see if there is actually a relationship between the magnetic moment and the spin polarization of a subset of the electronic states, we calculate both the magnetic moment and the spin polarization using a tight-binding model. The band structure of an alloy is calculated self-consistently within the coherent potential approximation. The magnetic moments and the spin polarization of the density of states for different bands at the Fermi level can then be obtained from the band structure. It is found that when the *p* and *d* bands are included, the spin polarization of the density of states is obviously inconsistent with the experiments. For example, negative spin polarization is obtained for Ni when the *d* bands are included. Therefore, we present only the results of the spin polarization of the *s* electrons.

The alloys we consider are substitution alloys, in which some of the host atoms are replaced by impurity atoms without changing the crystal structure. The band structure of these alloys can be found by the coherent potential approximation.²³

Before the band structure calculation of a magnetic *3d* alloy can be carried out, one has to know the splitting between the majority and minority spins, which is related to the magnetic moment. The splitting can be found within our model from the number of majority and minority electrons, which has to be found from the band structure. Therefore, the band structure, the number of majority and minority electrons, and the splitting have to be solved self-consistently.

To calculate the alloy band structure, we consider a nine-band tight-binding Hamiltonian written as

$$H = \sum_{im\sigma} u_{im}^\sigma c_{im\sigma}^\dagger c_{im\sigma} + \sum_{\langle ij \rangle mn\sigma} t_{ijmn} c_{im\sigma}^\dagger c_{jn\sigma}, \quad (1)$$

where $c_{im\sigma}^\dagger$ ($c_{im\sigma}$) is the creation (annihilation) operator of a spin- σ electron of orbital m on the lattice site i , u_{im}^σ is the on-site potential, t_{ijmn} is the hopping energy between neighbors. The band structure of the alloy described by this Hamiltonian will be found using the coherent potential approximation. Tight-binding parameters in the Slater-Koster two-center form are obtained from fits to the local density approximation band structure.²⁴ In principle all of the parameters in the alloy are changed as one varies the alloy composition. However, the $3d$ alloys are similar and the differences in hopping and s and p on-site energies are not as significant as the differences in the d on-site energies. Therefore, we assume that the most important changes due to alloying are contained in the on-site energies, $u_{i,d}^\uparrow$ and $u_{i,d}^\downarrow$, of the spin-up (majority) and spin-down (minority) d electrons. In other words, the alloy is assumed to have site-independent hopping parameters and s and p on-site energies the same as the host metal, and site-dependent d on-site energies. This assumption will be justified later by the agreement with local density calculations of supercells in different impurity concentrations.

The major contributions to the on-site energies, $u_{i,d}^\uparrow$ and $u_{i,d}^\downarrow$ come from the atomic core potential plus the Coulomb energy due to the opposite spin. In the itinerant electron model, it is more convenient to work with the number of spin-up and spin-down d electrons, $N_{i,d}^\uparrow$ and $N_{i,d}^\downarrow$, at each site i . Therefore, we rewrite the parameters in the form of

$$\begin{aligned} u_{i,d}^\uparrow &= U_i^0 + U_i^x N_{i,d}^\downarrow \\ u_{i,d}^\downarrow &= U_i^0 + U_i^x N_{i,d}^\uparrow, \end{aligned} \quad (2)$$

where U_i^0 and U_i^x are the on-site parameter and effective Coulomb energy per pair at site i . Both $N_{i,d}^\uparrow$ and $N_{i,d}^\downarrow$ in Eq. (2) are obtained from the band structure, which in turn depends on $u_{i,d}^\uparrow$ and $u_{i,d}^\downarrow$. Thus, Eq. (2) has to be solved self-consistently with the band structure calculated from the Hamiltonian of Eq. (1).

All parameters for the host atoms can be found from fits to the local density calculations of the pure metal.²⁴ The only two parameters left, U_{imp}^0 and U_{imp}^x of impurity atoms, are obtained from fits to the local density calculations of supercells composed the two types of atoms. For example, parameters for Fe as impurities in fcc Ni host are obtained from fits to fcc Ni₃Fe band structures. As a check, parameters obtained from the fit is used to calculate the tight-binding band structure of fcc Ni₃₁Fe, which agrees with the local density approximation band structure. This indicates that the model works well at least when impurity concentration is less than 25%. When the impurity concentration is large, or when the difference in hopping between the host and the impurity is large, the

error is expected to increase. Although this simplified model requires only two more parameters in addition to the parameters of the host, it still produces correctly the Slater-Pauling curve for the magnetic moment²⁵.

The three quantities which we will compare are the magnetic moment per atom, the polarization of the density of states as measured by tunneling experiments, and the polarization of the calculated s density of states. The magnetic moment per atom, μ , is determined from the number of electrons per atom in the majority spin orientation, N^\uparrow , and the minority spin orientation, N^\downarrow , via

$$\mu = \mu_B (N^\uparrow - N^\downarrow), \quad (3)$$

where μ_B is the Bohr magneton. The s density of states of spin σ at the Fermi level at lattice site i is defined as

$$n_{i,s}^\sigma = \int \frac{d^3\mathbf{k}}{(2\pi)^3} \delta(E_F - E(\mathbf{k})) \sum_{m=1}^9 |\langle is\sigma | \mathbf{k} m \sigma \rangle|^2, \quad (4)$$

where $|is\sigma\rangle$ is the s orbital with spin σ at site i and $|\mathbf{k} m \sigma\rangle$ is the m -th eigenvector with a wavevector \mathbf{k} and spin σ . The net s density of states is the weighted average of the s density of states at each lattice site:

$$n_s^\sigma = (1/N_{at}) \sum_i n_{i,s}^\sigma, \quad (5)$$

where N_{at} is the number of atoms in the sample. The density of states for spin σ measured experimentally is denoted by n^σ . Using these definitions, the polarization of the tunneling density of states, P , and the calculated s density of states, P_s , are given by

$$P = \frac{n^\uparrow - n^\downarrow}{n^\uparrow + n^\downarrow}, \quad (6)$$

$$P_s = \frac{n_s^\uparrow - n_s^\downarrow}{n_s^\uparrow + n_s^\downarrow}. \quad (7)$$

IV. RESULTS

As mentioned, when the density of states of the p and d bands are included, the spin polarization is inconsistent with experiments. Therefore, to compare with the experiments, we plot the spin polarization of the s density of states, P_s , against the calculated magnetic moment in the same graph as the experimental data. In Fig. 4, we plot the calculated spin polarization of NiCr and NiCu (filled symbols), together with the experimental tunneling spin polarization, P , shown in Fig. 2 (unfilled symbols). We choose to calculate NiCr and NiCu because they represent different dependencies of the magnetic moment on the average number of electrons. As seen in Fig. 1(b), the magnetic moment of NiCr increases as the average number of electrons increases, while the the magnetic moment

of NiCu decreases as the average number of electrons increases. For both alloys, the calculated spin polarization varies from zero (non-magnetic) to about 27% (pure Ni), and has the same dependency on the magnetic moment. When the magnetic moment is zero, the majority and minority spin bands are the same, and the spin polarization are also zero.

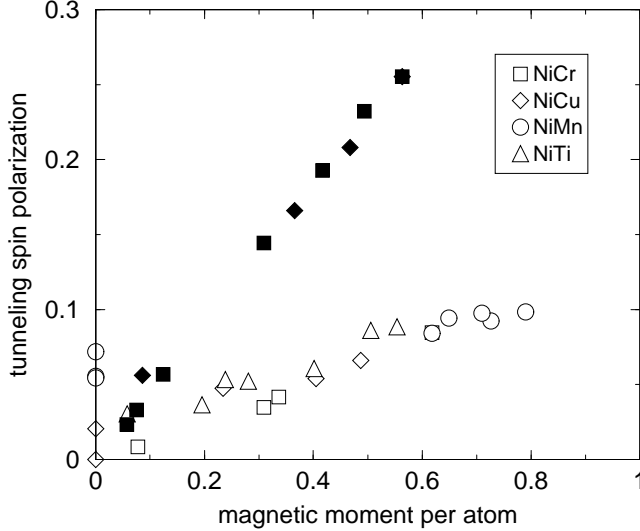


FIG. 4. Calculated spin polarization of the s density of states of NiCr (filled square) and NiCu (filled diamond) alloys versus the magnetic moment plotted with the experimental data (open symbols) shown in fig 2. The spin polarization measured for these series of films are lower than the calculated values. One reason is that a growth technique that seems to reduce the spin polarization was used in order to mix the elements. For example, the tunneling spin polarization measured for the Ni films in the series are only about 8%, which is much lower than the values of 27 – 33% measured for the Ni films grown by better techniques.

Both calculated and experimental results show that the spin polarization is positive and roughly proportional to the magnetic moment. However, the experimental values are much lower than the calculated ones. One reason may be that in order to mix the elements, the samples in this series of experiments were grown with technique which seems to reduce the spin polarization.¹⁰ For example, the tunneling spin polarization measured for the Ni films in this series is only about 8%, which is much lower than the measured values of 27 – 33% for the Ni films grown by better techniques.^{10,8}

To compare with more experiments, we plot in Fig. 5 the calculated spin polarization of the s electrons for NiCr, NiCu, and fcc and bcc NiFe (filled symbols) together with the experimental spin polarization shown in Fig. 3 (unfilled symbols). As explained above, the calculation for the lower left regime agrees with the tunneling experiment. The calculation for the middle regime (fcc NiFe) agrees well with the tunneling experiments and the Andreev reflection experiments by Upadhyay *et al.*, but not with the Andreev reflection experiments of Soulen *et*

al. and Nadgorny *et al.* In the right regime (bcc NiFe), the calculated results are significantly higher than the measured values.

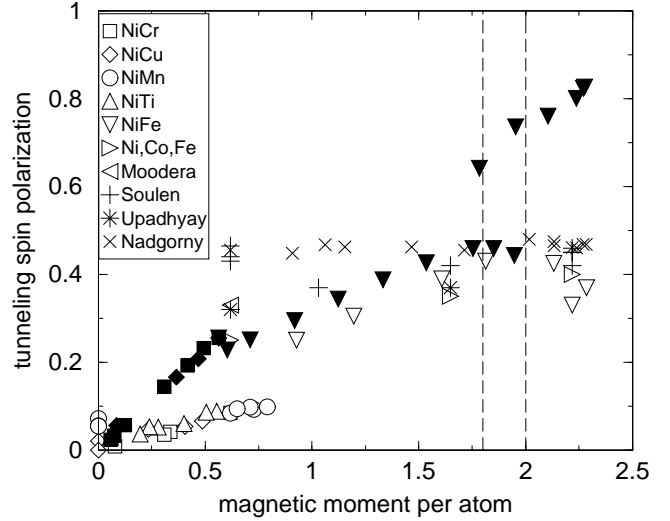


FIG. 5. Calculated spin polarization of the s density of states of NiCr (filled square), NiCu (filled diamond), and NiFe (filled downward triangle) alloys versus the magnetic moment plotted with the experimental data (open symbols) shown in Fig 3.

Thus far we have presented calculations of the bulk density of states. However, experiments have suggested that the spin-polarized tunneling electrons originate from the first two to three layers at the surface.^{4,10} To estimate how the surface affects the spin polarization, we study the variation of the s density of states as a function of depth from the surface. The band structure of bcc (100) Fe, hcp (001) Co, and fcc (111) Ni slabs of 18 atomic layers thick are calculated by using fixed tight-binding parameters. This calculation only serves as a crude estimate of the surface effects. Self-consistent iterations are not used in the band structure calculation. Effects such as the change in surface magnetic moment and surface roughness are also neglected. We study the spin polarization of the cumulative s density of states as a function of the number of layers. The cumulative s density of states of spin- σ in the first l layers from the surface is defined as $\bar{n}_{l,s}^\sigma = \sum_{j=1}^l n_{j,s}^\sigma$, where $n_{j,s}^\sigma$ is the s density of states in the j -th layer. The spin polarization of the cumulative s density of states for the first l layers from the surface is given by

$$\bar{P}_{l,s} = \frac{\bar{n}_{l,s}^\uparrow - \bar{n}_{l,s}^\downarrow}{\bar{n}_{l,s}^\uparrow + \bar{n}_{l,s}^\downarrow}. \quad (8)$$

This quantity is related to the tunneling spin polarization because it takes into account the electrons contributed from the first few layers. However, this is only an approximation to the tunneling spin polarization because the contribution from different layers may not be uniformly weighted.

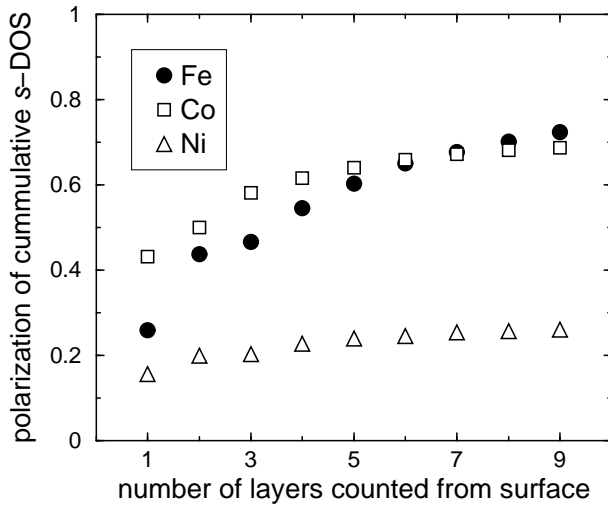


FIG. 6. Calculated spin polarization of the cumulative s density of states, $\overline{P}_{l,s}$, as a function of the number layers counted from the surface. We studied the spin polarization of the cumulative s density of states because tunneling may be sensitive to the first few layers. As shown in the graph, the spin polarization of the s density of states at the bcc Fe surface is significantly lower than that in the bulk. This reduction is less important in the hcp and fcc metals. Therefore, our estimation of the tunneling spin polarization using the bulk spin polarization is good for the fcc metals, while it is too large in the case of the bcc metals, as shown in fig 5.

As shown in Fig. 6, there is a reduction of the spin polarization near the surface. The reduction is more important in bcc metals than in fcc metals. For example, the spin polarization of bcc Fe surface is less than one third of the bulk value, while the spin polarization of the fcc Ni surface is about two thirds of the bulk value. The degree of reduction in the spin polarization depends mainly on the structure of film. Therefore, as seen in Fig. 5, our calculation for the spin polarization of the bcc alloys using the bulk spin polarization is significantly higher than the experimental value, which may be related to the surface spin polarization. For the same reason, the calculated spin polarization of the fcc alloys agrees well with the experiments.

One may now ask the question: why should the polarization of the s density of states, P_s , and the magnetic moment per atom, μ , be related? In Fig. 7 we have plotted the s density of states, $n_{i,s}^\sigma$, for the two spin orientations, σ , at the different sites, i , in fcc Ni rich alloys. The x-axis is the total number of electrons, N_i^σ , at site i with spin σ . As evident from the figure, for a range of compositions and different alloys, all the points lie on the same curve. The solid and dashed lines are obtained from pure Ni by varying the Fermi energy in the spin-up and spin-down bands respectively. This curve contains the key to understanding why the s density of states and the magnetic moment are related. In the range of $3.0 < N_i^\sigma < 5.5$, $n_{s,i}^\sigma$ is an *increasing* function of N_i^σ

for both spins. Since n_s^σ increases as N^σ increases, it follows that the spin polarization, $P_s \propto (n_s^\uparrow - n_s^\downarrow)$, increases with increasing magnetic moment, $\mu = \mu_B(N^\uparrow - N^\downarrow)$.

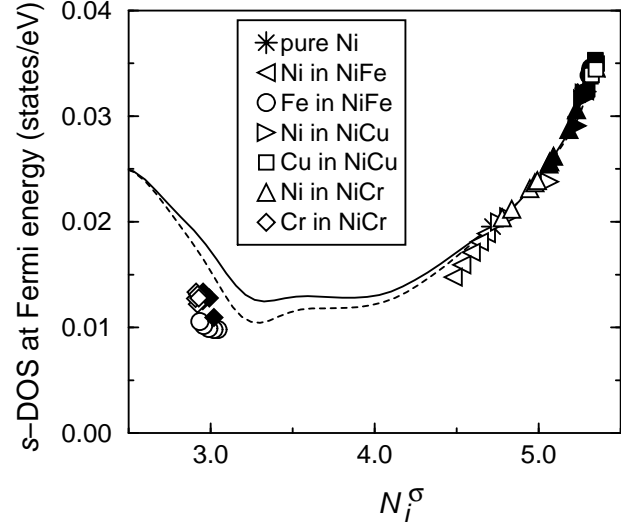


FIG. 7. The s density of states $n_{s,i}^\sigma$ at the Fermi energy for spin-up (filled symbols) and spin-down (unfilled symbols) channels versus the number of spin-up and spin-down valence electrons, N_i^\uparrow and N_i^\downarrow , at site i ($i = \text{Ni, Fe, Cu, ...}$) in fcc alloys. The solid (dashed) curve is obtained by varying the Fermi energy in the spin-up (spin-down) density of states of pure Ni. In the range of interest, ($N_i^\sigma > 3$) $n_{s,i}^\sigma$ is an increasing function of N_i^σ . It follows that $P_s \propto (n_s^\uparrow - n_s^\downarrow)$ increases as $\mu = \mu_B(N^\uparrow - N^\downarrow)$ increases, explaining the correlation in Fig. 1-3.

It is important to note that P_s is only roughly proportional to μ because the curve in Fig. 7 is quite different from a straight line even in the range of $3.0 < N_i^\sigma < 5.5$. Furthermore, this is not a universal relation because the curve shown in Fig. 7 is for the fcc Ni rich alloys. Other kinds of alloys would presumably produce a different curve, possibly even a decreasing instead of an increasing curve. For example, applying the same analysis to bcc alloys such as FeCr shows that the s density of states is still an increasing function of N_i^σ in the range of interest. However, as shown in Fig. 8, a much different curve is obtained for the bcc alloys. In bcc alloys, the s density of states has sudden jumps in the energy range of interest. One of the jumps is reflected in Fig. 8 by the curves near $N_i^\sigma = 4.5$. The jump causes a sudden increase in the spin polarization of the s density of states in bcc FeCr with low Fe concentration,²⁵ which has not been studied experimentally.

While this explains the correlation, it still leaves open the question of why all the Ni rich alloys fall on a single curve in Fig. 7 and why that curve is increasing. To understand this we examine more closely the band structure and in particular the density of states for the s and d bands. The d density of states is responsible for the magnetic moment, while as argued above the s density

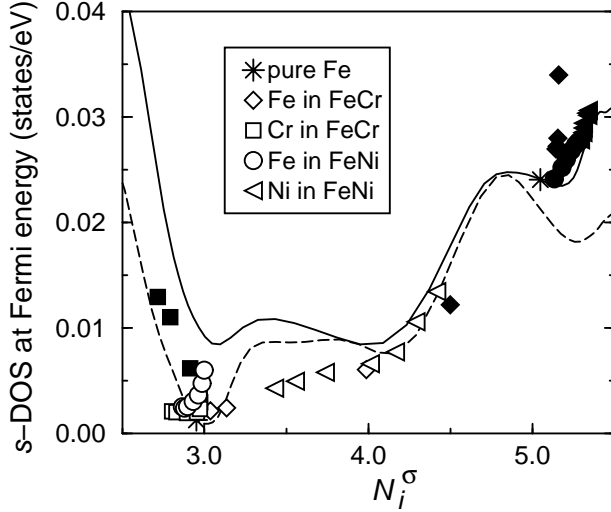


FIG. 8. The s density of states $n_{s,i}^\sigma$ at the Fermi energy for spin-up (filled symbols) and spin-down (unfilled symbols) channels versus the number of spin-up and spin-down valence electrons, N_i^\uparrow and N_i^\downarrow , at site i ($i = \text{Ni, Fe, or Cr}$) in bcc alloys. The solid (dashed) curve is obtained by varying the Fermi energy in the spin-up (spin-down) density of states of pure Fe. In this case, $n_{s,i}^\sigma$ is still an increasing function of N_i^σ in most region; however, the function is more complicated than that of the fcc alloys.

of states is responsible for the tunneling. The s and d density of states are related by s - d hybridization.

As an example, we have plotted in Fig. 9 the s and d density of states near the Fermi level for (a) the majority band and (b) the minority band at the Ni sites of pure Ni, $\text{Ni}_{0.8}\text{Fe}_{0.2}$, and $\text{Ni}_{0.6}\text{Fe}_{0.4}$. We have shifted the energy such that within the same spin channel, the integrated density of states from the bottom of the bands to 0 eV (*not* the Fermi level) are the same for every alloy. The Fermi energies in these plots are indicated by the vertical lines. The s density of states fall on the same curve and the d peaks have the same energy. The only difference among the alloys are the Fermi levels. Thus, the primary effect of alloying at the Ni sites is to shift the s and d bands *together* relative to the Fermi level. We see from Fig. 9 that the s density of states n_s^σ of the fcc alloys is an increasing function of the Fermi energy in the range where the Fermi level lies. On the other hand, N^σ , the integrated density of states up to the Fermi level, also increases with the Fermi energy. Therefore n_s^σ is an increasing function of N^σ as shown in Fig. 7.

It should be noted that the shifting of the d bands is due to energy considerations as in the itinerant electron theory. It results in the change of the magnetic moments, μ . On the other hand, the shifting of the s band is due to its hybridization with the shifted d bands. It results in the change of the spin polarization of the s density of states, P_s .

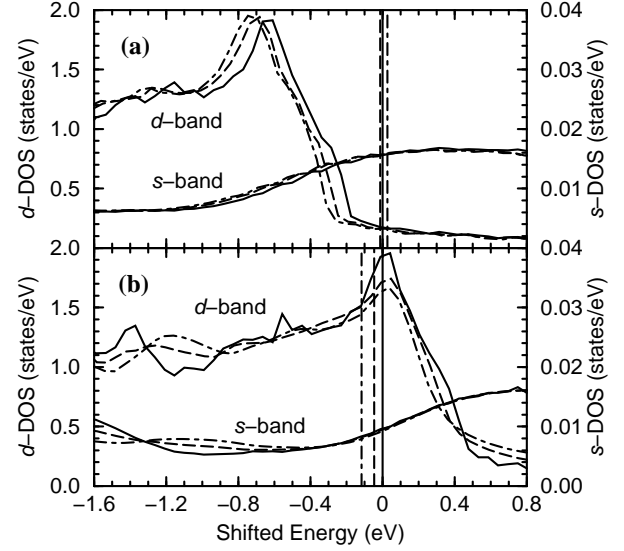


FIG. 9. The (a) spin-up and (b) spin-down d and s density of states at the Ni sites in pure Ni (solid lines), $\text{Ni}_{0.8}\text{Fe}_{0.2}$ (dashed lines) and $\text{Ni}_{0.6}\text{Fe}_{0.4}$ (dot-dashed lines) versus the shifted energies. The energy of each spin channel for each alloy is shifted such that the number of states at the Ni sites below 0 eV is the same as pure Ni in the corresponding spin channel. The d peaks roughly coincide and the s density of states collapse onto a single curve. Therefore the primary effect of alloying is to shift the bands together relative to the Fermi level. This explains why data for different alloys and spins in Fig. 7 are on the same curve. The positive slope in Fig. 7 can be explained by noting that the Fermi levels lie in the range where the s density of states increases as a function of energy and hence the number of electrons N_i^σ .

V. CONCLUSION

In this paper, a microscopic calculation for both the magnetic moment and the spin polarization of subsets of the density of states of the 3d alloys are studied. By interpreting the tunneling spin polarization as the spin polarization of the s density of states, the trends in the tunneling experiments of Tedrow and Meservy are obtained. The correlation between the magnetic moment and the density of states are understood by showing that the s density of states for both spin orientations is an increasing function of the number of electrons and by showing that the primary effect of alloying is to shift the bands together relative to the Fermi level. The correlation between the magnetic moment and the polarization of the s density of states is not universal. All of this work supports the picture that the tunneling current is dominated by s electrons.

While we have explained the correlation between the spin polarization and the magnetic moment, there are still a number of open questions. Within this model, the tunneling current is assumed to be dominated by s electrons, but the mechanism behind it is not clear. Tsymbal and Pettifor²¹ suggested that the hopping from the d

bands of the ferromagnet to the s band of the barrier is essentially zero. In $3d$ metals, the s - d hopping is normally a few times smaller than the s - s hopping, so it is reasonable to assume a similar ratio for the hopping at the metal-insulator interface. However, we note that since the d density of states is about two orders of magnitude higher than that of the s density of states at the Fermi level, the s - d hopping has to be much smaller than a tenth of the s - s hopping to explain the dominance of the tunneling current by the s electrons. Therefore, it is unclear if such a requirement is physical.

In another model, suggested by Nguyen-Manh *et al.*,²² the s band in the insulator is spin-polarized by the d band of the ferromagnet due to hybridization, causing a positive spin polarization in the s current. The model predicts that in the insulator there is very small but spin polarized density of states at the Fermi level.

On the other hand, a different model was suggested by Mazin¹⁷ and Nadgorny *et al.*¹⁸ They argued that the current, both in tunneling and Andreev reflection experiments, is proportional to the density of states times the Fermi velocity squared. The low(high) density of states of the $s(d)$ electrons are therefore compensated by their high(low) Fermi velocities. Thus, both the s and the d electrons are important to the tunneling current. The spin polarization they calculated is roughly independent of the magnetic moment, much like the Andreev reflection data the group obtained. At this point, it is unclear which of the above models gives a better physical picture.

Another open question is whether the spin polarization measured by the tunneling experiments and the Andreev reflection point contact experiments are the same. Mazin¹⁷ and Nadgorny *et al.*¹⁸ argued that the two are the same. However, the situation here is more complicated. There are even disagreements among the results obtained from the Andreev reflection experiments. The results obtained by Soulen *et al.*¹⁵ and Nadgorny *et al.*¹⁸ are not the same as those obtained by Upadhyay *et al.*¹⁶ It is unclear whether this is due to the differences in the sample preparation or the method of data analysis.

There are also qualitative differences between the prediction of different models. While our calculations show that the spin polarization increases with magnetic moments, the calculations by Mazin¹⁷ and Nadgorny *et al.*¹⁸ show that the spin polarization is independent of the magnetic moments. However, the spin polarization can remain constant at most in a certain regime. In regimes such as $\text{Ni}_{1-x}\text{Cr}_x$ with $x > 0.15$, $\text{Ni}_{1-x}\text{Cu}_x$ with $x > 0.55$, or the invar regime near $\text{Ni}_{0.36}\text{Fe}_{0.64}$, the magnetic moment drops to zero. When the magnetic moment is zero the spin polarization is expected to be zero because there is no difference between the majority and minority spins. It would be helpful to compare experiments and theories in these regimes.

- ¹ M. N. Baibich *et al.*, Phys. Rev. Lett. **61**, 2472 (1988).
- ² M. Johnson, Phys. Rev. Lett. **70**, 2142 (1993); Science **260**, 320 (1993).
- ³ S. Jin *et al.*, Science **264**, 413 (1994).
- ⁴ R. Meservey and P.M. Tedrow, Phys. Rep. **238**, n.4, 173 (1994).
- ⁵ M. Julliere, Phys. Lett. **50A**, n.3, 225 (1975).
- ⁶ S. Maekawa and U. Gafvert, IEEE Trans. Magn. **MAG-18**, 707 (1982).
- ⁷ T. Miyazaki and N. Tezuka, J. Magn. Magn. Mater. **139**, L231 (1995).
- ⁸ J. S. Moodera *et al.*, Phys. Rev. Lett. **74**, 3273 (1994); Phys. Rev. Lett. **80**, 2941 (1998).
- ⁹ S. Zhang *et al.*, Phys. Rev. Lett. **79**, 3744 (1997).
- ¹⁰ P. M. Tedrow and R. Meservey, Phys. Rev. Lett. **26**, n.4, 192 (1971); R. Meservey, D. Paraskevopoulos, and P.M. Tedrow, Physica **91B**, 91 (1977); D. Paraskevopoulos, R. Meservey, and P.M. Tedrow, Phys. Rev. B **16**, 4907 (1977).
- ¹¹ J. C. Slater, J. Appl. Phys. **8**, 385 (1937).
- ¹² J. Friedel, Nuovo Cimento 10 Suppl. no. 2, **VII**, 287 (1958)
- ¹³ J. Crangle and G. C. Hallam, Proc. R. Soc. London Ser. A **272**, 119 (1963).
- ¹⁴ P. H. Derichs *et al.*, Journ. Magn. Magn. Mat. **100**, 241 (1991).
- ¹⁵ R. J. Soulen *et al.*, Science **282**, n.5386, 85 (1998).
- ¹⁶ S. K. Upadhyay *et al.*, Phys. Rev. Lett. **81**, 3247 (1998).
- ¹⁷ I. I. Mazin, cond-mat/9812327.
- ¹⁸ B. Nadgorny *et al.*, cond-mat/9905097.
- ¹⁹ M. B. Stearns, Phys. Rev. B **8**, 4383 (1973).
- ²⁰ J. A. Hertz and K. Aoi, Phys. Rev. B **8**, 3252 (1973).
- ²¹ E. Yu. Tsybal and D. G. Pettifor, J. Phys.: Condens. Matter **9**, L411 (1997).
- ²² D. Nguyen-Manh *et al.*, Mat. Res. Soc. Symp. Proc. **492**, 319 (1998).
- ²³ R. J. Elliott, J. A. Krumhansl, and P. L. Leath, Rev. Mod. Phys. **46**, 465 (1974).
- ²⁴ D. A. Papaconstantopoulos, *Handbook of the band structure of elemental solids*, (Plenum Press, New York, 1986).
- ²⁵ T.-S. Choy, J. Chen, S. Hershfield, J. Appl. Phys. **86**, 562 (1999).